

A Data-driven Adversarial Examples Recognition Framework via Adversarial Feature Genome

Li Chen

Central South University

School of Geosciences and Info-Physics

vchenli@csu.edu.cn

Qi Li

Central South University

School of Computer and Engineering

dsjliqi@csu.edu.cn

Jian Peng

Central South University

School of Geosciences and Info-Physics

PengJ2017@csu.edu.cn

Hailun Ding

Central South University

School of Computer and Engineering

dh1317618@gmail.com

Jiawei Zhu

Central South University

School of Geosciences and Info-Physics

jw_zhu@csu.edu.cn

Haifeng Li*

Central South University

School of Geosciences and Info-Physics

lihaifeng@csu.edu.cn

Abstract

Convolutional neural networks (CNNs) are easily spoofed by adversarial examples which lead to wrong classification results. Most of the defense methods focus only on how to improve the robustness of CNNs or to detect adversarial examples. They are incapable of detecting and correctly classifying adversarial examples simultaneously. We find that adversarial examples and original images have diverse representations in the feature space, and this difference grows as layers go deeper, which we call Adversarial Feature Separability (AFS). Inspired by AFS, we propose a defense framework based on Adversarial Feature Genome (AFG), which can detect and correctly classify adversarial examples into original classes simultaneously. AFG is an innovative encoding for both image and adversarial example. It consists of group features and a mixed label. With group features which are visual representations of adversarial and original images via group visualization method, one can detect adversarial examples because of AFS of group features. With a mixed label, one can trace back to the original label of an adversarial example. Then, the classification of adversarial example is modeled as a multi-label classification trained on the AFG dataset, which can get the original class of adversarial example. Experiments show that the proposed framework not only effectively detects adversarial examples from different attack algorithms, but also correctly classifies adversarial examples. Our framework

potentially gives a new perspective, i.e., a data-driven way, to improve the robustness of a CNN model.

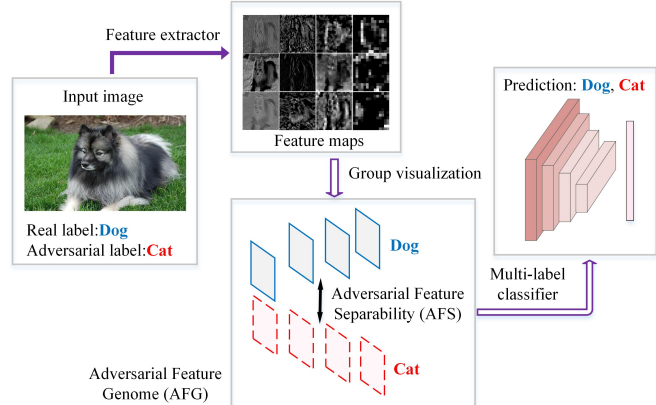


Figure 1: The input image is an adversarial example, and its real label is a dog. It is misclassified as a cat by the trained CNN. In our framework, we use the trained CNN to extract the original image into an AFG. This AFG preserves the class features, including the property of AFS. We use AFG dataset to train a multi-label classifier to detect this adversarial example and classifies the input image correctly.

1. Introduction

Convolutional neural networks (CNNs) achieve remarkable success in a variety of tasks [5, 12, 14, 8]. However, Szegedy and others [9, 29, 4, 16, 6] find that an original image would be misclassified with high confidence via adding a very small perturbation to it, which is called adversarial example. Adversarial examples show that CNNs suffer serious robustness problem even though good performance.

There are two main types of defense algorithms for adversarial examples [1]. One is called the complete defense which makes the model recognize adversarial example as the correct class [10, 31]. For instance, Papernot [25] applies knowledge distillation to transfer knowledge of complex models to simple networks, and then classifies adversarial examples through simple networks. This method only defends against small perturbation attacks. Gradient masking [30] makes the network be in unreachable states on the gradient to prevent adversarial examples generation. When under a stronger attack [2], the defendant will be broken through and it has a highly complex computation. The other is detection only [33, 32, 19] which sends an alarm to potential adversarial examples to reject any further processing. These methods use different image patterns from model processing to detect adversarial examples. However, these patterns cannot retain the class features. They cannot know the original class of the image, and only reject all potential adversarial examples. In summary, it is a challenge to a defensive algorithm to detect adversarial examples and classify them correctly. The basic reason is we do not have an effective way to measure the difference between adversarial example and original image in the feature space.

Our experiments show that the difference of feature maps of adversarial examples and original images gradually becomes separable as the layers go deeper. We theoretically analyze and verify this phenomenon, and call it Adversarial Feature Separability (AFS). The AFS is a potential metric to measure the change of adversarial example in the feature space, which provides an insight that adversarial examples can be detected in feature space. However, we need to acquire the class features which have the representations of the class to get the real class of adversarial example. The group visualization method proposed by Olah [24] provides a feasible way to interpret the internal representations of CNNs by group features. We find these group features contain the representations corresponding to the class of the input image.

In this paper, we combine the above two ideas and propose an Adversarial Feature Genome (AFG) data organized by stacking the stitched groups features of different layers. AFG is encoded with representations of an image or adversarial example of the model, which consists of group features and a mixed label. These group features allow AFG to detect adversarial example. The mixed label of each AFG

indicates its original label and a dynamic label. These two labels are consistent for original images, but are different for adversarial examples. This label encoding allows AFG to be classified into the corresponding class. We transform all images into AFGs to construct a big dataset. Finally, we trained a multi-label classifier on the AFG database. The multi-label classifier effectively detects adversarial examples from the original images and also correctly classifies them. This recognition framework is shown in Figure 1. The experiments demonstrate that under a variety of attack algorithms, the proposed framework has a good defensive ability in different models and correctly obtains the original label of adversarial example. Our contributions are summarized as follows:

- We discover that adversarial examples and original images can be measured in the feature space, which we called Adversarial Feature Separability (AFS). Moreover, we observe that AFS become more obvious as the layers go deeper.
- We create AFG data which contains group features with AFS and a mixed label. It builds the foundation for correctly classify adversarial example, and also provides a new way for model interpretability.
- The multi-label classifier trained on the AFG dataset can recognize adversarial examples. To the best of our knowledge, this is the first framework that can detect and correctly classify adversarial examples simultaneously. This framework provides a new perspective to design defensive attack algorithms.

2. Adversarial Feature Separability

To detect adversarial example, we need to know that the difference between adversarial and original image. Adversarial example by adding attack noise to the input allows the model to give a false classification result with high confidence [29]. Goodfellow [9] points out that linearity in high-dimensional space is the reason to cause adversarial example. Due to the under-fitting of the image space by the linear portion of the deep model, the cumulative error has an effect on the final result. However, we find that in the feedforward of the same model for images and adversarial examples, the difference of their feature maps is obvious with the deepening of the layers, which we call Adversarial Feature Separability (AFS).

First, we use neural networks to show the impact of attack noise on the feedforward of the model. We define X as the original image, and its label is y . ρ is attack noise, which is generated by optimization algorithms such as gradient descent. This attack noise is highly targeted to the model and belongs to a white-box attack. Adversarial example ($X + \rho$)

can be defined by Eq.1.

$$\min_{\rho} \|\rho\|_2 \quad s.t. \quad f(X + \rho) = \hat{y}. \quad (1)$$

Adversarial example $(X + \rho)$ makes the neural network misclassify it into class \hat{y} . $f(\cdot)$ represents the classifier of the neural network. The weights and biases of the first layer of the neural network are defined as W and b . The difference between adversarial example and the original image before the activation function is as follows:

$$(WX + b) - (W(X + \rho) + b) = W\rho. \quad (2)$$

Despite both W and ρ are high-dimensional data, it is not certain that $W\rho$ brings errors. However, the classification results show that $y \neq \hat{y}$, and \hat{y} has high confidence. This also means that the distribution of results before y and \hat{y} is quite different. The error of $W\rho$ is passed from the first layer to the last layer. The error is not reduced in the feedforward of the neural network.

In CNNs, models have many convolution kernels, and each convolutional kernel is used to extract a feature map. The output feature maps of the convolution layer are the input of the next convolution layer. They influence the final inference. As with neural network analysis, the feedforward of CNNs also causes differences on each layer's feature maps due to attack noise. This shows that there are differences in the feature space between the two input images, but it does not reflect that the difference will gradually separate, that is, AFS. To measure whether there is AFS in this difference, we define P_i as the feature maps of original image in the i -th layer, \hat{P}_i as the feature maps of adversarial examples, and $D(P_i \parallel \hat{P}_i)$ denotes a distance function of P_i and \hat{P}_i . The distance between feature maps at each layer can be defined as

$$D(P_i \parallel \hat{P}_i) = \frac{\|P_i - \hat{P}_i\|}{\|P_i\|}, \quad (3)$$

where $\|\cdot\|$ represents the Eular norm. We also apply KL divergence [11] to measure the difference between the distribution of P_i and \hat{P}_i in Eq.4.

$$D_{KL}(P_i \parallel \hat{P}_i) = \sum \mu_j(P_{ij}) \log \frac{\mu_j(P_{ij})}{\mu_j(\hat{P}_{ij})}, \quad (4)$$

where P_{ij} represents the feature map obtained by j -th convolution kernel in the i -th layer, and $\mu_j(P_{ij}) = \sum P_{ij} / \sum P_i$ is the empirical distribution through discrete samples. Then, we generate some adversarial examples on GoogleNet [28] with several attack algorithms, including Fast Gradient Sign Method (FGSM) [9], Basic Iterative

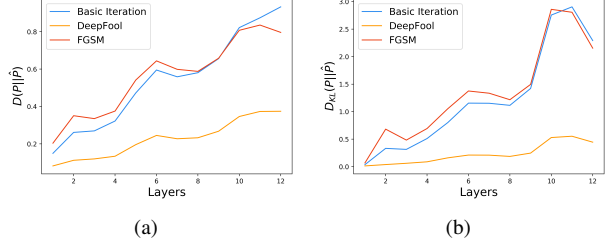


Figure 2: (a) Distance difference and (b) KL divergence to measure the difference between adversarial example and original image on each layer under different attack algorithms. (a) and (b) show that as the layer becomes deeper, the difference in the feature maps becomes larger for all attack algorithms, which means that adversarial example and the original image can be separated.

Methods (BIM) [13], and DeepFool [22]. We randomly choose 100 classes from the ImageNet dataset, and each class includes 200 images. The result of the experiment is shown in Figure 2.

As shown in Figure 2, two measurement methods demonstrate that the feature maps of adversarial examples obtained by different attack algorithms are different from those of the original images on each layer. This difference is small in the shallow layers, but increases with the deepening of layers. The images and adversarial examples have the property of AFS in the feature space. Their differences gradually become larger as the layers go deeper. Liao [17] verified that when the input was added random noise, and this difference did not change significantly with layer changes. Therefore, attack noise is the cause of AFS, not random noise.

3. Adversarial Feature Genome

The basic structure of Adversarial Feature Genome (AFG) is that the group features of the input image on each layer are obtained by the group visualization method. These group features not only have the property of AFS, but also represent different features of the input image, like gene expression. Besides, AFG has a mixed label of real and adversarial classes. These two parts of AFG ensure that adversarial example can be classified.

3.1. Group Features

The AFS can be used to detect adversarial examples, but this property does not allow the model to classify adversarial examples. We need to get the class features while the adversarial features are separated. Olah [24] proposes a group visualization method. This method can visualize the features of the input image on each layer into several important group features. These group features can be used as

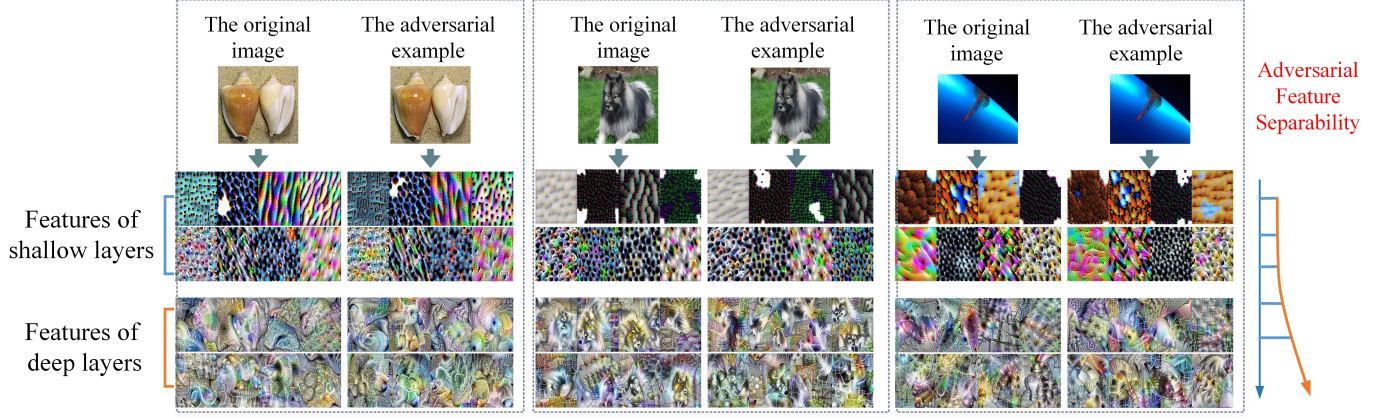


Figure 3: The three sets of images and corresponding adversarial examples are conch and teddy, dog and cat, jellyfish and paper towel. We get the group features of each input image on each layer of the model. In the shallow layers, group features of adversarial examples and original images are similar but they differ in the deeper layers. Meanwhile, this difference also reflects AFS.

class features of the input image.

In detail, for input image X , P_i is the feature maps in the i -th layer. It is a 4D tensor (Batch, Width, Height, Channel), and Batch = 1. The dimension of P_i is high and contains many redundant features. These redundant features have little effect on the classification of X . To get meaningful features, we need to reduce the dimensions of P_i . First, we convert P_i to $P_{i(W \times H), C}$. This means that each feature maps of the layer are converted into column vectors and merged into a matrix, and the matrix is a non-negative matrix. Then, non-negative matrix factorization (NMF) [15] is applied on $P_{i(W \times H), C}$ to reduce dimensions. We want to find non-negative matrix factors U and V such that:

$$P_{i(W \times H), C} \approx (UV)_{(W \times H), C} = \sum_{a=1}^r U_{(W \times H), a} V_{a, C}, \quad (5)$$

where r represents the number of the group. Finally, we apply activation maximization algorithm [7] on each group to obtain the group features X_{ij}^* as follows:

$$X_{ij}^* = \arg \max h_{ij}(U_{(W \times H), j} V_{j, C}, \Theta^*), \quad (6)$$

where $h_{ij}(X, \Theta^*)$ is the value of the j -th group in the i -th layer, and Θ is the weight set of CNN. The obtained image X_{ij}^* , an important group feature on the i -th convolution layer, makes the maximum activation of the j -th group on the i -th layer. We visualize 3 pairs of adversarial example and the original image shown in Figure 3. The group features of adversarial examples and the original images are similar in the shallow layer, but the difference in the deep layer becomes larger. Meanwhile, according to the change

of the adversarial features, the features of adversarial examples and the original images are gradually separated. These group features have the properties of AFS, and the details can be seen in Experiment 5.2.

Group features are simple in shallow, but complex in deep layers. In the deeper layers, features tend to become more abstract and closer to semantic features. In each class, objects have common features, such as the hair and ears of a dog, the tip of a bird, and the spherical cap of a jellyfish. The group features on each layer of the image show the classification of the image of the model. It is like the process of gene expression, using the information in genes to synthesize gene products. Many visualization methods and analysis of the model [23, 34, 3] also prove that these semantic features are obvious in the deep layer. These group features have class features of the input image, and the details can be seen in Experiment 5.3.

3.2. AFG Data Structure

The input image X gets r group features on each layer, r denotes the number of groups. For instance, we choose $r = 4$, and the size of X_{ij}^* is 112×112 . Each layer generates 4 group features of 112×112 . We stitch four group features together on the same layer to get a larger feature 224×224 . Then the large features of all layers that become a tensor $224 \times 224 \times N$ are stacked together. N represents the number of layers. This tensor is the AFG of the input image. AFG preserves the spatial relationship between features while preserving the features of each layer.

When the model classifies adversarial example, the original image is misclassified into other classes due to attack noise. In this process, the adversarial features gradually deviate from the original features, and the original features of

Original	One-hot	Misclassified	One-hot	Final Label
cat	10	cat	000	10000
cat	10	jellyfish	100	10100
cat	10	conch	010	10010
dog	01	dog	000	01000
dog	01	jellyfish	100	01100
dog	01	sturgeon	001	01001

Table 1: Cat and dog are labels for images. Jellyfish, conch and sturgeon are adversarial labels. In the original image, label '10' represents a cat and '01' represents a dog. In adversarial example, the label '100' represents the jellyfish, '010' represents the conch, and '001' represents the squid. When the cat image is misclassified as jellyfish, the AFG label of the image is '10100'.

the image have been transferred to other classes. From the original class to the wrong class, we give AFG a mixed label. One label is the correct class, and the other is the class of the model misclassified. The two labels of AFG of the original image are correct class.

The mixed label of AFG is a one-hot encoding. We first count the number of classes for all images and the number of classes for adversarial examples. Moosavi [21] shows the distance between the classes of the images and the classes of adversarial examples. The number of original classes and adversarial classes may not be the same. Simply, the total number of classes is twice the number of original classes. After determining the encoding length of the original labels and the adversarial labels, one-hot encoding is used for each of the two types of labels. The two labels of each AFG are joined into a vector which is the final label of the AFG. The encoding examples are shown in Table 1.

4. Data-driven Adversarial Examples Recognition Framework

We call the framework a data-driven adversarial examples recognition. The whole framework contains two classifiers, as shown in Figure 4. The first classifier is trained on the original dataset to do a classification task. When the first model is trained, adversarial examples are obtained from the first classifier by the different attack algorithms. We get the AFGs of all images via the first trained model. All AFGs form a new dataset, and we turn the defense and classification of adversarial examples into a multi-label classification problem. A multi-label classifier trained on the AFG datasets to detect adversarial examples. The second multi-label classifier can choose a variety of algorithms, and the results of different multi-label classifiers are shown in Experiment 5.5.

AFG has labels for two classes. According to the confidence of the two labels, the predicted results can reconfirm

the original classification results. When the two labels are inconsistent, the image is an adversarial example. The distribution of the final prediction result can detect the original label and misclassified label.

5. Experiments

5.1. Experimental Setup

The data-driven adversarial example recognition framework requires two classifiers. In the experiment, we mainly use two configurations, the first classification model selects VGG16 [26] and GoogleNet [29] respectively, and the second model uses VGG16. That is VGG16+VGG16 and GoogleNet+VGG16. We randomly selected 100 classes on the ImageNet dataset, each with 200 images, as the dataset for the first model. For the trained model, we use the FGSM [9], BIM [13], and DeepFool [22] attack algorithms to obtain adversarial examples. Then we convert all images into the AFG dataset. The second model is trained on the AFG dataset. We use the SGD optimizer, which has a learning rate of 0.001 and iterations of 500 epochs.

When training the first model, we fine-tune it on 100 classes through the pre-trained model. The final accuracy of VGG16 is 89.81%, and the accuracy of GoogleNet is 91.23%. In the FGSM and BIM algorithms, the change part is multiplied by a coefficient ϵ to make the attack noise small, and $\epsilon = 0.005$. We use the update strategy of L_∞ metrics in BIM with a total of 100 iterations. The L_∞ version of the DeepFool attack is adopted, and it takes 80 iterations.

We first validate group features of AFG have AFS property and the class features, which is the foundation of the framework. Then, we use different strategies to analyze the recognition of AFGs under the second classifiers and the results of multiple multi-label classifiers.

5.2. The AFS of AFGs

Since the AFS property of AFG is important, we first need to verify that the classifier based on the AFG dataset can detect adversarial example. We turn the second model into a binary classification, and simplify the coding of AFG label. A simplified label indicates that the AFG is from an original image or adversarial example. The results of the second model are compared with Detector algorithm. It is a detection only method proposed by Metzen [20]. This method proposes a small "detector" to distinguish between real data and adversarial example. It uses an extra model to detect adversarial example as our method, but its method does not correctly classify adversarial example. We use two configurations with different attack algorithms, and the result is shown in Table 2.

The results in Table 2 show that among the three attack algorithms, the accuracy of adversarial examples obtained

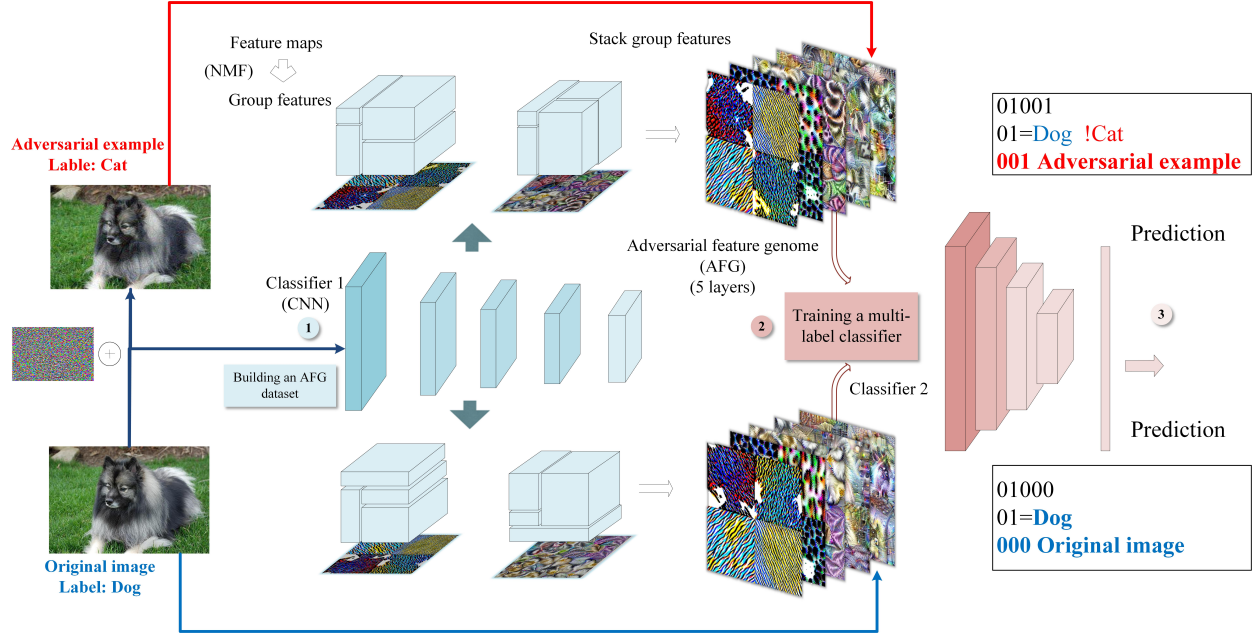


Figure 4: A data-driven adversarial example recognition framework. After the training of the first classification model, the framework can be divided into three steps. (1) We use the first classifier CNN to convert the input image into group features by the group visualization method. (2) We stack all stitched group features to create an AFG for each input image. The number of AFG channels is the same as the number of convolution layers. We construct a dataset from AFGs of all images. (3) The defensive adversarial example is transformed into a multi-label classification problem. The second multi-label classifier is trained on the AFG dataset. It can detect whether the input image is an adversarial example and the correct class of adversarial example.

Configuration	Method	AFG	Detector
VGG16+VGG16	FGSM	93.75%	89.01%
	BIM	88.32%	87.14%
	DeepFool	74.42%	82.13%
GoogleNet+VGG16	FGSM	88.94%	91.01%
	BIM	93.41%	88.21%
	DeepFool	72.44%	79.33%

Table 2: In both configurations, we use different attack algorithms to verify the AFS of AFG, which is the ability to distinguish between images and adversarial example. The results are also compared with detector algorithm.

by DeepFool algorithm, whether AFG or detector, can be correctly classified by the second model is relatively low. For the FGSM and BIM algorithms, the accuracy of AFG and detector is close. AFG can distinguish genuine image from data containing adversarial examples.

In the VGG16+VGG16 configuration, the AFG obtained by the FGSM algorithm better detects adversarial example, while for the GoogleNet+VGG16 configuration, the AFG obtained under the BIM algorithm better detects adversarial

examples. This may be due to structural differences in the first model that causes the difficulty of generating adversarial examples. Liu [18] suggested that it was more difficult to get an adversarial example on VGG16. Olah [24] also stated that the group features of GoogleNet were more semantic and easier to understand than that of VGG16 [23].

This experiment shows that AFG does reserve the AFS property to ensure this representation can distinguish adversarial examples and original images.

5.3. The Class Features of AFGs

The AFG gets the original class of adversarial example, which requires AFG to retain the feature difference and also includes the class features of the corresponding input image. We change all AFGs converted from genuine images into single labels. Each label has the same class as the corresponding input image. The second model is trained on this dataset to do a multi-class classification. The experimental results of the two configurations are shown in Table 3.

The results show that the second model under two configurations has a good accuracy in recognizing AFG classes. Compared with the first model, their accuracy rate has decreased. Although AFG contains the features of the in-

Configuration	Accuracy
VGG16+VGG16	78.31%
GoogleNet+VGG16	81.12%

Table 3: We train two sets of models on the original AFG dataset. Each AFG has a label with the same of the input image. The model is trained on the dataset to perform the classification task to verify the class features of AFG.

put image, it is synthesized by several group features compressed by the features on the layer. Compression of features brings losses and errors. Besides, the AFG generation is related to the first model, and AFG may contain information about the first model. The number of channels of the obtained AFG is related to the number of the layers of the first model. A large number of channels increase the complexity of the AFG. These factors make AFG of each input image lose the features of the input image and increase the training difficulty of the second model.

This experiment shows that AFG contains the class features of the input image, which helps the multi-label classifier learn the AFG class while distinguishing adversarial example.

5.4. The Recognition of AFGs

The AFS and class features of AFG ensure that the AFG of adversarial example is potentially classified correctly. We use all AFGs, including original images and adversarial examples, as the dataset for the second multi-label classifier. The two classes with the highest confidence in the prediction result are compared with the two classes of the AFG label. We choose intersection over union (IoU) to evaluate the performance of the second multi-label model. The results are shown in Table 4.

Method	VGG16+VGG16	GoogleNet+VGG16
FGSM	49.41%	72.71%
BIM	52.12%	71.63%
DeepFool	55.62%	65.18%

Table 4: The performance of adversarial example recognition under different attack algorithms.

From the results, the multi-label classifier can get the correct and misclassified classes of adversarial example. However, under attack algorithms, the recognition of GoogleNet+VGG16 is better than that of VGG16+VGG16. In the VGG16+VGG16 configuration, the best result is to detect adversarial examples obtained by DeepFool, and the worst is adversarial examples from FGSM. This result is contrary to the result of the GoogleNet+VGG16 configuration. In GoogleNet+VGG16 configuration, the worst result

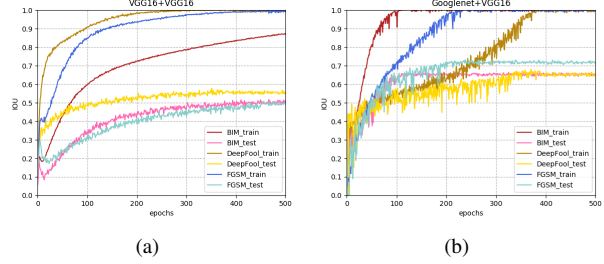


Figure 5: (a) and (b) are training of AFGs obtained from different attack algorithms under different configurations.

is for DeepFool, and the best is to classify adversarial examples from FGSM. We analyze the training process as shown in Figure 5.

Under the three attack algorithms, the converge of GoogleNet+VGG16 is fast and the test result is higher. The VGG16+VGG16 is not easy to converge. In the DeepFool algorithm, compared with adversarial examples from VGG16, adversarial examples of GoogleNet are difficult to distinguish. However, in the GoogleNet+VGG16 configuration, it can better defend the DeepFool algorithm. According to the previous experimental analyses, the structural differences of the models can make a great difference in the generation of adversarial examples.

Besides, we find that for the same configuration, the IoU under different attack algorithms is close. To explore the generalization of the multi-label classifier obtained by one attack algorithm on other attack algorithms for the same configuration, we use the multi-label classifier obtained under different attack algorithms to test the AFGs built on other attack algorithms. The experimental results are shown in Table 5.

Configuration	Method	FGSM	BIM	DeepFool
VGG16 +VGG16	FGSM	49.41%	31.14%	30.33%
	BIM	37.65%	52.12%	34.87%
	DeepFool	42.53%	42.12%	55.62%
GoogleNet +VGG16	FGSM	72.71%	85.64%	82.03%
	BIM	85.22%	71.63%	81.31%
	DeepFool	85.54%	86.61%	65.18%

Table 5: Generalization of multi-label classifier obtained by an attack algorithm on other attack algorithms.

From Table 5, for the GoogleNet+VGG16 configuration, the multi-label classifier trained on any attack algorithm is equal or better than that of the other two attack algorithms. For the VGG16+VGG16 configuration, the results of the trained multi-label classifier on the other two attack algorithms are lower. This shows that multi-label classifier is generalized to other attack algorithms. This generalization

Method	FGSM(1)	BIM(1)	DeepFool(1)
FGSM(2)	56.78%	45.66%	49.87%
BIM(2)	44.21%	34.90%	55.21%
DeepFool(2)	53.65%	48.43%	61.46%

Table 6: Generalization of multi-label classifier obtained by an attack algorithm on other model.

is related to attack algorithms and the first model. To further explore this generalization to defend other attack algorithms, we use multi-label classifier obtained under (2) the GoogleNet+VGG16 configuration to detect AFGs under (1) the VGG16+VGG16 configuration. The result is shown in Table 6. This result shows that even the multi-label classifier obtained under another configuration, it still has generalization when detecting adversarial examples of other models, which provides a new idea for exploring the transfer and universality of adversarial examples.

	All	Original Only	Adversarial Only
AFG	71.63%	61.59%	84.61%
AFG-F3L3	62.21%	52.02%	86.64%
AFG-FML	68.77%	58.02%	85.42%
AFG-F3	60.32%	60.81%	82.47%
AFG-L3	67.31%	51.54%	85.08%

Table 7: Performance of different channel AFGs.

In the experiment, we use the all channels of AFG. While AFG in different channels contains different features, they may have different effects on defending adversarial examples. In the BIM algorithm under the GoogleNet+VGG16 configuration, we choose the first three layers and the last three layers of the AFG data (AFG-F3L3), the first/middle/last data (AFG-FML), the first only data (AFG-F3), and the last only data (AFG-L3). On these datasets, the multi-label classifier is trained to verify all the AFG dataset, the real AFG dataset and the adversarial AFG dataset. The results show that the IoU of the multi-label classifier from the AFG-FML dataset decreases a little (Table 7). When testing different types of data, full channel AFG is better to detect real AFG data. For the adversarial AFG dataset, it is better to select multi-label classifier from the AFG-FML dataset. In the case of comparisons of AFG-F3 and AFG-L3, the multi-label classifier from the AFG-L3 dataset can better recognize the real AFG data, and the AFG-L3 dataset can help classifier recognize the adversarial AFG data. The results show that the AFG data can select different channels for different application scenarios, which also can effectively reduce the computational complexity of AFG.

This experiment shows that the difficulty of AFG recognition is related to the attack algorithms and the first model

Configuration	IoU
GoogleNet+VGG16	71.63%
GoogleNet+GoogleNet	52.12%
GoogleNet+SVM	35.58%

Table 8: Performance of different multi-label classifiers.

structure. The multi-label classifier obtained under different attack algorithms has generalization ability against various attacker. We also can selectively use the channel of AFG.

5.5. The different multi-label classifiers

The adversarial example recognition framework relies on a second multi-label classifier to detect adversarial examples, and the choice of the second model is flexible. Different classifiers have different defensive abilities. Besides VGG16, we chose other classifiers as the second model, including GoogleNet and SVM [27].

We use GoogleNet as the first model, and the AFG dataset obtained by the BIM algorithm is used as the dataset of the second model training. The results are shown in Table 8. The recognition results of AFG by different classifiers vary greatly. The result of the VGG16 to detect adversarial examples is good, while the SVM results are the worst.

The results show that the deep model is better than the shallow model on classifying AFG into the real class. This may because that AFG has a large dimension and contains complex features, and it makes the second model more difficult to converge, especially for shallow models like SVM.

GoogleNet should be able to converge on this dataset well, but the results differ greatly from VGG16. In the course of training, the training curve of GoogleNet fluctuates greatly and converges slowly. This is in sharp contrast to the training process of VGG16. As in the second section of the experimental analysis, the group features of GoogleNet and VGG16 differ greatly in semantics, and the difficulty of generating adversarial examples varies. The reason for the poor results of AFG classification by GoogleNet may be related to the structure of the model.

This experiment shows that the flexibility of the second classifier selection. Without changing the first model, we can defend against multiple attack algorithms. The second model can even improve the final result by learning multiple multi-label models through ensemble learning.

6. Discussion and Conclusion

In this paper, we propose a new paradigm, i.e. data driven paradigm, for adversarial example defending methods. This paradigm is built on the fact we observed: the original image and adversarial example are gradually separated in feature space, i.e. AFS. Inspired by AFS, We build

AFG which consists of group features and a mixed label. It can help classifier to detect adversarial examples and trace its original label. We transform images and adversarial example into the AFG dataset, and turn an adversarial examples defending problem into a multi-label classification problem. The multi-label classifier trained on the AFG dataset can get the original label of adversarial example and has generalization for other attack algorithm. The second model and the channel of AFG can also be applied flexibly. Our framework potentially gives a new perspective to defense adversarial examples.

In future works, we will encode the AFG database with more variables such as the architecture and hyperparameters of CNN models, to train a more universal model which has strong robustness to adversarial examples generated by different methods.

References

- [1] N. Akhtar and A. Mian. Threat of adversarial attacks on deep learning in computer vision: A survey. *IEEE Access*, 6:14410–14430, 2018.
- [2] A. Athalye, N. Carlini, and D. Wagner. Obfuscated gradients give a false sense of security: Circumventing defenses to adversarial examples. *arXiv preprint arXiv:1802.00420*, 2018.
- [3] D. Bau, J.-Y. Zhu, H. Strobelt, B. Zhou, J. B. Tenenbaum, W. T. Freeman, and A. Torralba. Gan dissection: Visualizing and understanding generative adversarial networks. *arXiv preprint arXiv:1811.10597*, 2018.
- [4] N. Carlini and D. Wagner. Audio adversarial examples: Targeted attacks on speech-to-text. *arXiv preprint arXiv:1801.00634*, 2018.
- [5] J. Deng, W. Dong, R. Socher, and L. J. Li. Imagenet: A large-scale hierarchical image database. In *Computer Vision and Pattern Recognition, 2009. CVPR 2009. IEEE Conference on*, pages 248–255, 2009.
- [6] G. F. Elsayed, D. Krishnan, H. Mobahi, K. Regan, and S. Bengio. Large margin deep networks for classification. *arXiv preprint arXiv:1803.05598*, 2018.
- [7] D. Erhan, Y. Bengio, A. Courville, and P. Vincent. Visualizing higher-layer features of a deep network. 2009.
- [8] L. Fei-Fei, R. Fergus, and P. Perona. One-shot learning of object categories. *IEEE transactions on pattern analysis and machine intelligence*, 28(4):594–611, 2006.
- [9] I. J. Goodfellow, J. Shlens, and C. Szegedy. Explaining and harnessing adversarial examples. *arXiv preprint arXiv:1412.6572*, 2014.
- [10] S. Gu and L. Rigazio. Towards deep neural network architectures robust to adversarial examples. *arXiv preprint arXiv:1412.5068*, 2014.
- [11] J. M. Joyce. Kullback-leibler divergence. *International encyclopedia of statistical science*, pages 720–722, 2011.
- [12] A. Krizhevsky, I. Sutskever, and G. E. Hinton. Imagenet classification with deep convolutional neural networks. In *Advances in neural information processing systems*, pages 1097–1105, 2012.
- [13] A. Kurakin, I. Goodfellow, and S. Bengio. Adversarial examples in the physical world. *arXiv preprint arXiv:1607.02533*, 2016.
- [14] Y. Lecun, Y. Bengio, and G. Hinton. Deep learning. *Nature*, 521(7553):436, 2015.
- [15] D. D. Lee and H. S. Seung. Algorithms for non-negative matrix factorization. *Advances in neural information processing systems*, 2001.
- [16] S. Li, A. Neupane, S. Paul, C. Song, S. V. Krishnamurthy, A. K. R. Chowdhury, and A. Swami. Adversarial perturbations against real-time video classification systems. *arXiv preprint arXiv:1807.00458*, 2018.
- [17] F. Liao, M. Liang, Y. Dong, T. Pang, X. Hu, and J. Zhu. Defense against adversarial attacks using high-level representation guided denoiser. In *Proceedings of the IEEE Conference on Computer Vision and Pattern Recognition*, pages 1778–1787, 2018.
- [18] Y. Liu, X. Chen, C. Liu, and D. Song. Delving into transferable adversarial examples and black-box attacks. *arXiv preprint arXiv:1611.02770*, 2016.
- [19] D. Meng and H. Chen. Magnet: a two-pronged defense against adversarial examples. In *Proceedings of the 2017 ACM SIGSAC Conference on Computer and Communications Security*, pages 135–147. ACM, 2017.
- [20] J. H. Metzen, T. Genewein, V. Fischer, and B. Bischoff. On detecting adversarial perturbations. *arXiv preprint arXiv:1702.04267*, 2017.
- [21] S.-M. Moosavi-Dezfooli, A. Fawzi, O. Fawzi, and P. Frossard. Universal adversarial perturbations. In *Proceedings of the IEEE Conference on Computer Vision and Pattern Recognition*, pages 1765–1773, 2017.
- [22] S.-M. Moosavi-Dezfooli, A. Fawzi, and P. Frossard. Deepfool: a simple and accurate method to fool deep neural networks. In *Proceedings of the IEEE Conference on Computer Vision and Pattern Recognition*, pages 2574–2582, 2016.
- [23] C. Olah, A. Mordvintsev, and L. Schubert. Feature visualization. *Distill*, 2(11):e7, 2017.
- [24] C. Olah, A. Satyanarayan, I. Johnson, S. Carter, L. Schubert, K. Ye, and A. Mordvintsev. The building blocks of interpretability. *Distill*, 3(3):e10, 2018.
- [25] N. Papernot, P. McDaniel, X. Wu, S. Jha, and A. Swami. Distillation as a defense to adversarial perturbations against deep neural networks. In *2016 IEEE Symposium on Security and Privacy (SP)*, pages 582–597. IEEE, 2016.
- [26] K. Simonyan and A. Zisserman. Very deep convolutional networks for large-scale image recognition. *arXiv preprint arXiv:1409.1556*, 2014.
- [27] J. A. Suykens and J. Vandewalle. Least squares support vector machine classifiers. *Neural processing letters*, 9(3):293–300, 1999.
- [28] C. Szegedy, W. Liu, Y. Jia, P. Sermanet, S. Reed, D. Anguelov, D. Erhan, V. Vanhoucke, and A. Rabinovich. Going deeper with convolutions. pages 1–9, 2015.
- [29] C. Szegedy, W. Zaremba, I. Sutskever, J. Bruna, D. Erhan, I. Goodfellow, and R. Fergus. Intriguing properties of neural networks. *arXiv preprint arXiv:1312.6199*, 2013.

- [30] F. Tramèr, A. Kurakin, N. Papernot, I. Goodfellow, D. Boneh, and P. McDaniel. Ensemble adversarial training: Attacks and defenses. *arXiv preprint arXiv:1705.07204*, 2017.
- [31] Q. Wang, W. Guo, K. Zhang, I. Ororbia, G. Alexander, X. Xing, X. Liu, and C. L. Giles. Learning adversary-resistant deep neural networks. *arXiv preprint arXiv:1612.01401*, 2016.
- [32] Y. Wang, H. Su, B. Zhang, and X. Hu. Interpret neural networks by identifying critical data routing paths. In *Proceedings of the IEEE Conference on Computer Vision and Pattern Recognition*, pages 8906–8914, 2018.
- [33] W. Xu, D. Evans, and Y. Qi. Feature squeezing: Detecting adversarial examples in deep neural networks. *arXiv preprint arXiv:1704.01155*, 2017.
- [34] M. D. Zeiler and R. Fergus. Visualizing and understanding convolutional networks. In *European conference on computer vision*, pages 818–833. Springer, 2014.